Autonomous Stabilization and Orientation Control of Hoisted Payloads

Brace W. White[1], Kyongchan Song[1], Iok Wong[1], and William R. Doggett[2]
NASA Langley Research Center, Hampton, VA 23681

Thomas C. Jones[3]
NASA Marshall Space Flight Center, Huntsville, AL 35812

An orientation control system prototype has been developed for hoisted payloads. This system will allow payloads to be lifted off inclined surfaces while maintaining orientation control, allowing removal of tightly packed payloads without colliding with adjacent objects. For this concept, the payload is hoisted with a crane using a rigging system composed of a cable routed through two capstans and three or four attachment points on the payload. Motors rotate the capstans to adjust the cable lengths to the payload, and thereby control the orientation of the payload. Initial testing of the prototype was completed using manual control, however the algorithms necessary to fully automate the system are presented in this paper.

Nomenclature

a_e, b_e, c_e	=	ellipsoid semiaxes
a_l, b_l, c_l	=	vector components of the parametric three-dimensional (3D) line equations
d	=	capstan diameter
F	=	force
h_0	=	initial height of the lift point above the payload when level
L	=	total cable length
l	=	box payload length
M	=	moment
m	=	slope of a line
n	=	cable segment/attachment point number
P_n	=	attachment point coordinates
P_0	=	lift point coordinates
r	=	cylinder payload radius
s_n	=	cable segment length
T_n	=	cable segment tension
t	=	center of gravity (CG) vector length required to intersect the semi-ellipsoid surface
$\widehat{u_n}$	=	cable segment direction/unit vector
W	=	payload weight
w	=	rectangle/box payload width
x, y, z	=	Cartesian coordinates
x_0, y_0, z_0	=	coordinates of CG
α, β, γ	=	roll, pitch, and yaw Euler angles
θ	=	angle between the bottom of the payload and the horizon in the two-dimensional (2D) model

I. Introduction

NASA and the space industry are currently developing lander systems to land a variety of payloads on the lunar surface. Lunar landers are designed to safely land on slopes inclined up to 15-degrees [1, 2]. Once the lander has settled on the lunar surface, many payloads the lander has transported will need to be relocated to the lunar surface or to mobility vehicles on the lunar surface. An efficient way to transfer payloads is to use a crane. Terrestrial cranes

[1] Research Aerospace Engineer, Structural Mechanics and Concepts Branch, AIAA Member
[2] Senior Research Engineer, Structural Mechanics and Concepts Branch, AIAA Associate Fellow
[3] Senior Research Engineer, Habitation Systems Development Office, AIAA Senior Member

often use ground personnel to help control payloads as they are relocated on cable supported hooks [3]. On the moon, an alternate approach is to use an automated lunar crane like the Lightweight Surface Manipulation System (LSMS) (Fig. 1) to lift payloads off an inclined lander deck [4]. However, ground personnel are not as readily available to help control the payloads and counteract swing. Swing will occur anytime the lifting force vector of the hoist system is not aligned with the weight vector of the payload, as a moment will be created about the lift point (Fig. 2). Swing is a concern because a lifted payload could collide with adjacent payloads on a crowded lander deck and cause critical damage (Fig. 3). A solution to this problem would be an actively controlled rigging system as is detailed below. The rigging system prevents swinging of cable attached loads and controls the orientation of the payload while in motion.

A prototype Auto-Rigging Payload Handling and Off-Loading System (ARPHOLS) [5] has been developed at NASA Langley Research Center to control payload orientation. Due to the COVID-19 pandemic, center access and laboratory resources were extremely limited. Those limitations led to the prototype being built from an available LEGO[*] Technic set and tested off-site (Fig. 4). The primary components of the ARPHOLS system are two motorized capstans, which can be rotated to adjust the position of a single continuous cable routed through a system of pulleys and attached to three or four points on the payload (Fig. 5). Since both ends of the cable are fixed, rotating the capstans changes the lengths of the different cable sections, thereby altering the orientation of the suspended payload. The motor controls for the LEGO prototype were programmed and transmitted sequentially via Bluetooth. Through several iteration cycles, the required degrees of rotation were determined to achieve predefined payload orientations to validate the concept for three and four attachment point configurations.

The ultimate vision for ARPHOLS is a fully automated rigging system, which can sense the incline angle of the lander deck, adjust the cable section lengths to match that angle, pick up and move the payload to the desired offload location while stabilized, adjust the orientation of the payload to match the offload location incline, and safely offload the payload (similar to the sequence shown in Fig. 6). To achieve automation, algorithms have been developed to calculate the leg lengths of cables attached to the payload and are presented in this paper.

II. Payload Orientation Control Algorithm Development

The first step in developing the control algorithms was to solve a simplified two-dimensional (2D) system (Fig. 7). A rectangle is chosen to represent the payload. The hoist cable has two attachment points at the top corners of the payload and one capstan at the lift point. As the capstan is rotated, the two cable sections change length, but the total cable length remains the same; during capstan rotation, while lifted, the lift point moves in an arc relative to the top of the payload. Following the arc from one extreme position to the other extreme position, the lift point traces a semi-ellipse with the two attachment points being the foci (Fig. 7). Gravity works to pull the payload into equilibrium, bringing the payload center of gravity (CG) directly below the lift point. Prior to lifting, the lift point can be strategically positioned directly above the payload CG, so the payload is already in equilibrium, thereby preventing swinging when lifted. While lifted into an area without obstacles, the lift point can be adjusted to change the orientation of the payload (for example to make the payload base parallel with the offloading surface). In this paper, the vertical axis on which the payload weight vector lies will be referred to as the "CG-axis". For a given payload orientation, the location of the lift point in relation to the top of the payload can be solved by finding the intersection of the CG-axis and the semi-ellipse if the location of the payload CG is known.

The process to find the intersection of the CG-axis and the semi-ellipse begins with the point-slope equation of a line

$$z - z_0 = m(x - x_0), \tag{1}$$

where x and z are cartesian coordinates in a frame attached to the payload with the origin located at the middle of the top surface, x_0 and z_0 are the coordinates of the CG, and m is the slope of the line. For this configuration, the slope is

$$m = -\cot\theta, \tag{2}$$

where θ is the angle between the bottom of the payload and the horizon. The equation for an ellipse [6] is

[*] The use of trademarks or names of manufacturers in this report is for accurate reporting and does not constitute an official endorsement, either expressed or implied, of such products or manufacturers by the National Aeronautics and Space Administration.

$$\frac{x^2}{a_e^2} + \frac{z^2}{b_e^2} = 1, \tag{3}$$

where a_e and b_e are the semiaxes of the ellipse (Fig. 8). The semiaxes are evaluated by geometric analysis. For example, if the lift point in Fig. 7b is extended to the maximum location along the *x*-axis, then there will be a certain length of doubled over cable that extends beyond the edge of the payload. This is an undesirable condition that would compromise the ability to control the orientation of the payload but can be avoided by properly positioning the payload lift points. To construct the ellipse, the distance beyond the edge of the payload can be determined by dividing the difference between the total cable length and the width of the payload by two. The distance from the origin to the maximum horizontal extension point can be determined by adding half the width of the payload to the distance beyond the edge of the payload. The vertical semiaxis can be evaluated with the Pythagorean theorem because the extended cable forms two mirrored right triangles when the lift points are symmetric about the axis location. The semiaxes for a two-point rectangular payload are

$$a_e = \frac{L}{2} \tag{4}$$

$$b_e = \frac{1}{2}\sqrt{L^2 - w^2}, \tag{5}$$

where L is the total length of the cable and w is the width of the payload. It can be shown that the lift point is then located at

$$x = \frac{1}{2(w^2 - L^2 \csc^2\theta)}\Big(-2L^2 \cot\theta\,(y_0 + x_0\cot\theta) + \sqrt{L^2(L-w)(L+w)(L^2 - w^2 - 4y_0^2 - 8x_0 y_0 \cot\theta + (L^2 - 4x_0^2)\cot^2\theta)}\Big) \tag{6}$$

$$z = \frac{1}{-2w^2 + 2L^2 \csc^2\theta}\Big(2L^2(y_0 + x_0\cot\theta) - 2w^2(y_0 + x_0\cot\theta) + \cot\theta\sqrt{L^2(L-w)(L+w)(L^2 - w^2 - 4y_0^2 - 8x_0 y_0 \cot\theta + (L^2 - 4x_0^2)\cot^2\theta)}\Big). \tag{7}$$

For the three-dimensional (3D) model, the rectangle payload becomes a rectangular box, a single cable is routed through four attachment points at the corners of the box, and there are two side-by-side motorized capstans at the lift point. Rotating the capstans changes the lengths of the different cable segments, and the lift point traces a semi-ellipsoid relative to the top of the payload (Fig. 9).

For a given payload orientation, the location of the lift point in relation to the top of the payload can be solved by finding the intersection of the CG-axis and the semi-ellipsoid. The CG vector and the semi-ellipsoid are initially defined in separate reference frames. The CG vector is chosen to be transformed to the reference frame of the semi-ellipsoid for simplicity. The CG vector is assumed to begin as a unit vector pointing in the positive *z*-direction from the gravity reference frame origin. Applying the general rotation matrix $R_z(\alpha)R_y(\beta)R_x(\gamma)$ to this unit vector yields the a_l, b_l, and c_l components of the parametric 3D line equations. The parametric 3D line equations [6] are

$$x = x_0 + a_l t \tag{8}$$

$$y = y_0 + b_l t \tag{9}$$

$$z = z_0 + c_l t, \tag{10}$$

where x_0, y_0, and z_0 are the coordinates of the CG *in the payload reference frame*. The payload reference frame is oriented with the payload, and the origin is located at the center of the top surface of the payload. The variable t is the required scalar length applied to the CG vector to intersect the semi-ellipsoid surface.

Applying the general rotation matrix $R_z(\alpha)R_y(\beta)R_x(\gamma)$ [7] to the CG unit vector

$$
\begin{bmatrix} \cos\alpha\cos\beta & \cos\alpha\sin\beta\sin\gamma - \sin\alpha\cos\gamma & \cos\alpha\sin\beta\cos\gamma + \sin\alpha\sin\gamma \\ \sin\alpha\cos\beta & \sin\alpha\sin\beta\sin\gamma + \cos\alpha\cos\gamma & \sin\alpha\sin\beta\cos\gamma - \cos\alpha\sin\gamma \\ -\sin\beta & \cos\beta\sin\gamma & \cos\beta\cos\gamma \end{bmatrix} \cdot \begin{bmatrix} 0 \\ 0 \\ 1 \end{bmatrix} = \begin{bmatrix} \cos\alpha\cos\gamma\sin\beta + \sin\alpha\sin\gamma \\ \cos\gamma\sin\alpha\sin\beta - \cos\alpha\sin\gamma \\ \cos\beta\cos\gamma \end{bmatrix} \tag{11}
$$

yields the rotated CG vector components

$$a_l = \cos\alpha\cos\gamma\sin\beta + \sin\alpha\sin\gamma \tag{12}$$

$$b_l = \cos\gamma\sin\alpha\sin\beta - \cos\alpha\sin\gamma \tag{13}$$

$$c_l = \cos\beta\cos\gamma, \tag{14}$$

where α, β, and γ are the roll, pitch, and yaw angles to achieve the required tilt.

The ellipsoid equation [6] is

$$\frac{x^2}{a_e^2} + \frac{y^2}{b_e^2} + \frac{z^2}{c_e^2} = 1, \tag{15}$$

where a_e, b_e, and c_e are the semiaxes (Fig. 10). The semiaxes are evaluated by geometric analysis, as was similarly done for the 2D model. Rather than using the total cable length as a variable, the initial height of the lift point above the payload surface when the payload is level, h_0, is used. The cable can be routed in many different configurations and several of the cable segments do not affect payload orientation, but rather support the cable routing. To simplify computation of the segment lengths affecting payload orientation, the initial lift point height is used instead of the total cable length. The semiaxes can be computed assuming a rectangular payload top with connections at the corners and are

$$a_e = \frac{\sqrt{h_0^2(4h_0^2+l^2)(4h_0^2+l^2+w^2)}}{4h_0^2+l^2} \tag{16}$$

$$b_e = \frac{\sqrt{h_0^2(4h_0^2+w^2)(4h_0^2+l^2+w^2)}}{4h_0^2+w^2} \tag{17}$$

$$c_e = h_0, \tag{18}$$

where l is the length and w is the width of the box.

The algorithms can be adapted to other payload geometries and number of attachment points by generating the semiaxes equations for each configuration. For example, the semiaxes for a four-point cylinder payload with evenly spaced attachment points at the circular edge of the top surface of the cylinder are

$$a_e = b_e = \frac{r}{\sqrt{2}} + \frac{2\sqrt{2}\sqrt{2h_0^6+3h_0^4r^2+h_0^2r^4} - 2\sqrt{2}h_0^2r - \sqrt{2}r^3}{2(2h_0^2+r^2)}, \tag{19}$$

where r is the radius of the cylinder. The closed-form values for the semiaxes for three-point-box and three-point-cylinder payloads are complex but can be solved rapidly numerically. Likewise, the location of the 3D lift point is solved numerically.

The length of each cable segment can be solved by calculating the distance from the corresponding attachment point to the lift point. The distance between two points is equal to the magnitude of the vector between the points, which is found by taking the norm of the vector. The vector between two points is found by subtracting the coordinates of the initial point from the final point.

$$\boldsymbol{s_n} = \overrightarrow{P_n P_0} = P_0 - P_n \tag{20}$$

$$s_n = |\boldsymbol{s_n}| = \left|\overrightarrow{P_n P_0}\right| \tag{21}$$

$$s_n = \sqrt{\left(P_{0,x} - P_{n,x}\right)^2 + \left(P_{0,y} - P_{n,y}\right)^2 + \left(P_{0,z} - P_{n,z}\right)^2}, \tag{22}$$

where $\boldsymbol{s_n}$ is the vector of cable segment n, s_n is the length of cable segment n, P_n is the Cartesian coordinates of attachment point n in the payload reference frame, and P_0 is the coordinates of the lift point. For a four-point-box payload, the coordinates of the attachment points are

$$P_1 = \left(\frac{l}{2}, \frac{w}{2}, 0\right) \tag{23}$$

$$P_2 = \left(-\frac{l}{2}, \frac{w}{2}, 0\right) \tag{24}$$

$$P_3 = \left(-\frac{l}{2}, -\frac{w}{2}, 0\right) \tag{25}$$

$$P_4 = \left(\frac{l}{2}, -\frac{w}{2}, 0\right), \tag{26}$$

where l is the length of the payload and w is the width of the payload.

The final step in the control system is to rotate the capstans the necessary amount to set the cable segment lengths. The arc length equation is

$$s = \frac{\varphi}{360}\pi d, \tag{27}$$

where s is the arc length, φ is the capstan rotation angle in degrees, and d is the diameter of the capstan. Setting the arc length to the required change in cable segment length Δs_n and solving for the capstan rotation angle yields

$$\varphi = 360\frac{\Delta s_n}{\pi d}. \tag{28}$$

Equation (28) is sufficient to set the lengths of cable segments one and four (Fig. 5a), but segments two and three are coupled, so a combination of sequential rotations from both capstans are required to achieve all the exact segment lengths. Further work is needed to fully develop the capstan rotation algorithms. Also, a z-axis rotatory actuator needs to be added to the system to account for the yaw angle of the incline.

An important aspect of the design of the system is choosing the material and thickness of the cable. That decision will depend on the expected tension loads in the cable segments. The tension in each cable segment can be solved using static analysis. When the system is in equilibrium, the sum of the forces and sum of the moments at any point equal zero. For a four-point box payload, the lift point is chosen as the analysis point in the gravity reference frame (so gravity points in the negative z-direction). Three force-sum equations (one in each direction) are created, which include the tension components in each cable segment. Since there are four unknown tensions, one additional moment-sum equation is required. The moments about the z-axis are chosen to be evaluated. Numerically solving the following equations results in the values of the tension in each cable segment

$$\sum F_x = 0$$

$$T_1\widehat{u_{1,x}} + T_2\widehat{u_{2,x}} + T_3\widehat{u_{3,x}} + T_4\widehat{u_{4,x}} = 0 \tag{29}$$

$$\sum F_y = 0$$

$$T_1\widehat{u_{1,y}} + T_2\widehat{u_{2,y}} + T_3\widehat{u_{3,y}} + T_4\widehat{u_{4,y}} = 0 \tag{30}$$

$$\sum F_z = 0$$

$$T_1\widehat{u_{1,z}} + T_2\widehat{u_{2,z}} + T_3\widehat{u_{3,z}} + T_4\widehat{u_{4,z}} - W = 0 \quad (31)$$

$$\sum M_z = 0$$

$$T_1\widehat{u_{1,x}}s_{1,y} + T_2\widehat{u_{2,x}}s_{2,y} + T_3\widehat{u_{3,x}}s_{3,y} + T_4\widehat{u_{4,x}}s_{4,y} + T_1\widehat{u_{1,y}}s_{1,x} + T_2\widehat{u_{2,y}}s_{2,x} + T_3\widehat{u_{3,y}}s_{3,x} + T_4\widehat{u_{4,y}}s_{4,x} = 0, \quad (32)$$

where T_n is the tension in cable segment *n*, $\widehat{u_n}$ is the direction/unit vector of cable segment *n*, W is the weight of the payload, and $s_{n,i}$ is the moment arm (i.e., vector component) of cable segment *n.*

III. MATLAB Design Tool and Graphical User Interface

The MATLAB* application designer tool was utilized to create a graphical user interface (GUI) to allow the user to experiment with different payload parameters and surface angles (Fig. 11). The GUI is interfaced to the background code and algorithm, which takes the input parameters and solves for the lift-point location, the lengths of each cable segment, and the tension in each cable segment. A simple 3D graphic of the payload is plotted, showing it suspended in the calculated orientation. The sliders for each parameter can be adjusted, and the plot is instantly updated with the new orientation. A future version of the app will accept the values of the parameters automatically and then rotate the capstans the required amount to achieve the desired orientation.

IV. Conclusion and Future Work

The ARPHOLS prototype has been validated to control payload orientation. The fundamental algorithms required to automate the system were presented in the paper and have been coded into a MATLAB application. After calculating the required lengths of each cable section with knowledge of the capstan diameter, the required degrees of rotation of each capstan can then be calculated to achieve the desired payload orientation. Further work is necessary to develop the capstan rotation algorithms. An updated prototype is being constructed, and a visual feedback system will be implemented to verify the control algorithms. The development of the ARPHOLS system is important for the advancement of space crane technology, as it will provide safe orientation control in lifting and offloading payloads.

References

[1] Suresh, A. K. and Srinivasan, T. P., "Potential Landing Sites for Chandrayaan-2 Lander in Southern Hemisphere of Moon," *49th Lunar and Planetary Science Conference*, The Woodlands, TX, March 2018.

[2] *Astrobotic Lunar Landers: Payload User's Guide*, Version 5.0, Astrobotic Technology, Inc., Pittsburgh, PA, August 2021, p. 51.

[3] Phillips, J., "The Use of Taglines to Control Crane Loads," Warren Forensics, published online January 2022. https://www.warrenforensics.com/2022/01/13/the-use-of-taglines-to-control-crane-loads/

[4] Jones, T. C., "A Protoflight Lightweight Surface Manipulation System to Enable High Load, Long-Reach Lunar Surface Operations," *2021 AIAA ASCEND Conference*, Las Vegas, NV, November 2021.

[5] Song, K., White, B., and Wong, I., "Verification and Validation of a Conceptual Model Using a LEGO Technic System and 3D Printed Parts," *2024 AIAA SCITECH Conference* abstract.

[6] Stewart, J., *Multivariable Calculus – Early Transcendentals*, 6th ed., Thomson Brooks/Cole, USA, 2008.

[7] Craig, J., *Introduction to Robotics: Mechanics and Control*, 2nd ed., Addison-Wesley, USA, 1989.

* The use of trademarks or names of manufacturers in this report is for accurate reporting and does not constitute an official endorsement, either expressed or implied, of such products or manufacturers by the National Aeronautics and Space Administration.

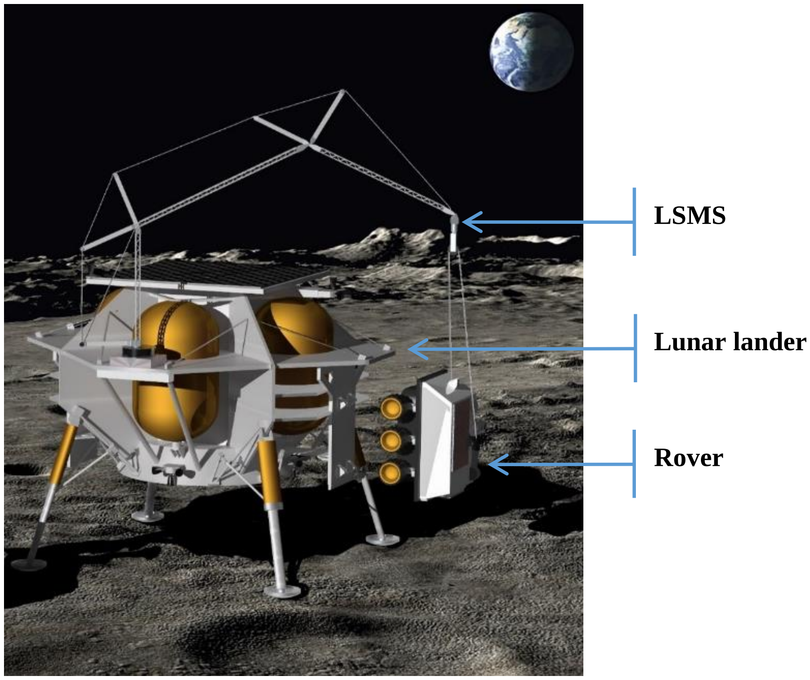

Figure 1. LSMS unloading a rover from a lunar lander.

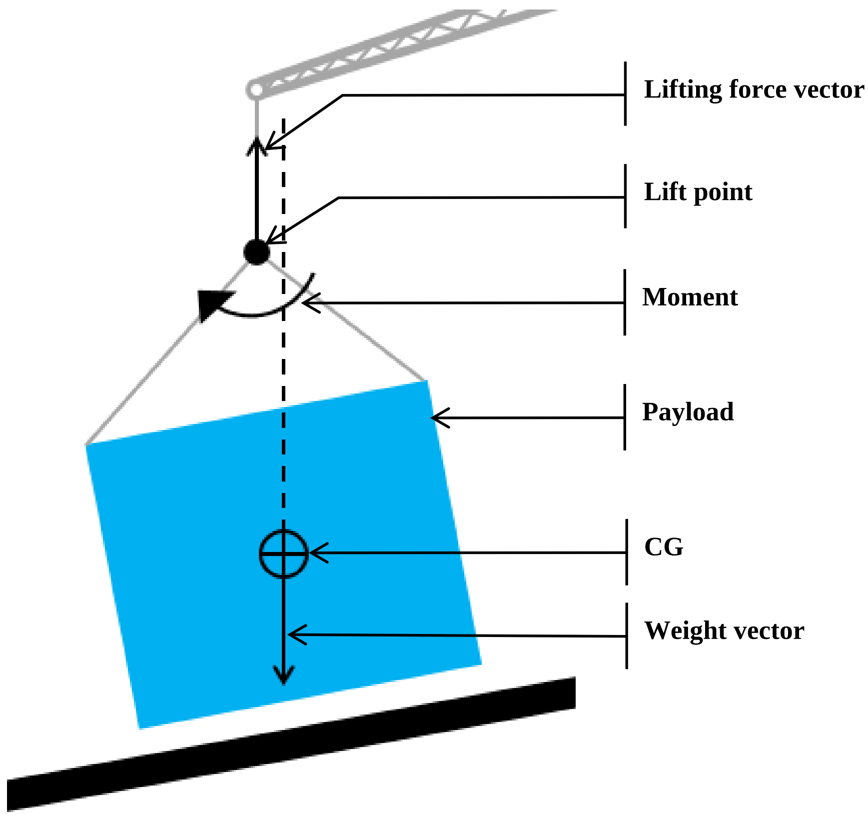

Figure 2. Moment due to misalignment of the lifting force and weight vectors.

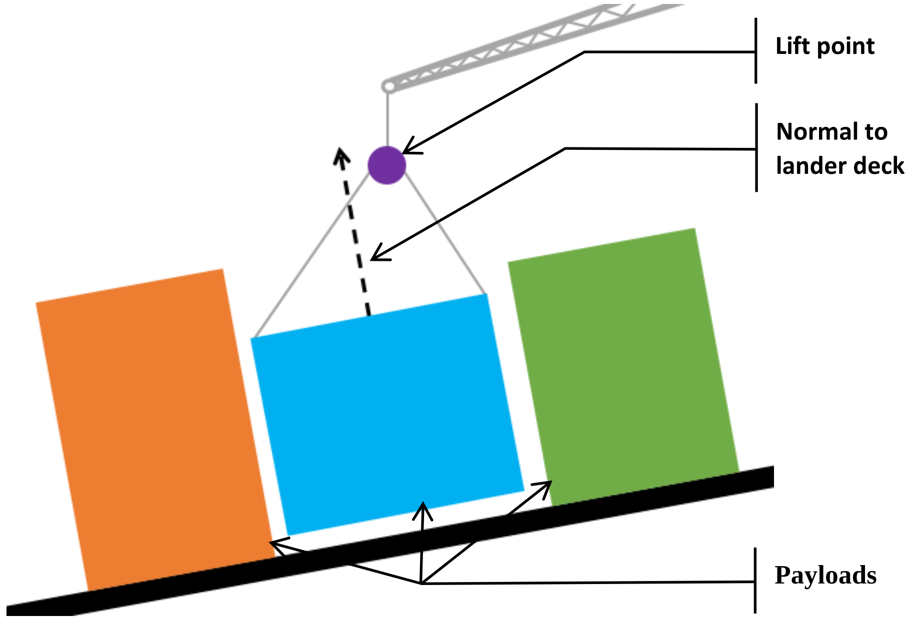

Figure 3. Payload being lifted off a crowded and inclined lander deck. The payload must be in equilibrium when lifted and move along a path normal to the lander deck to avoid colliding with adjacent payloads.

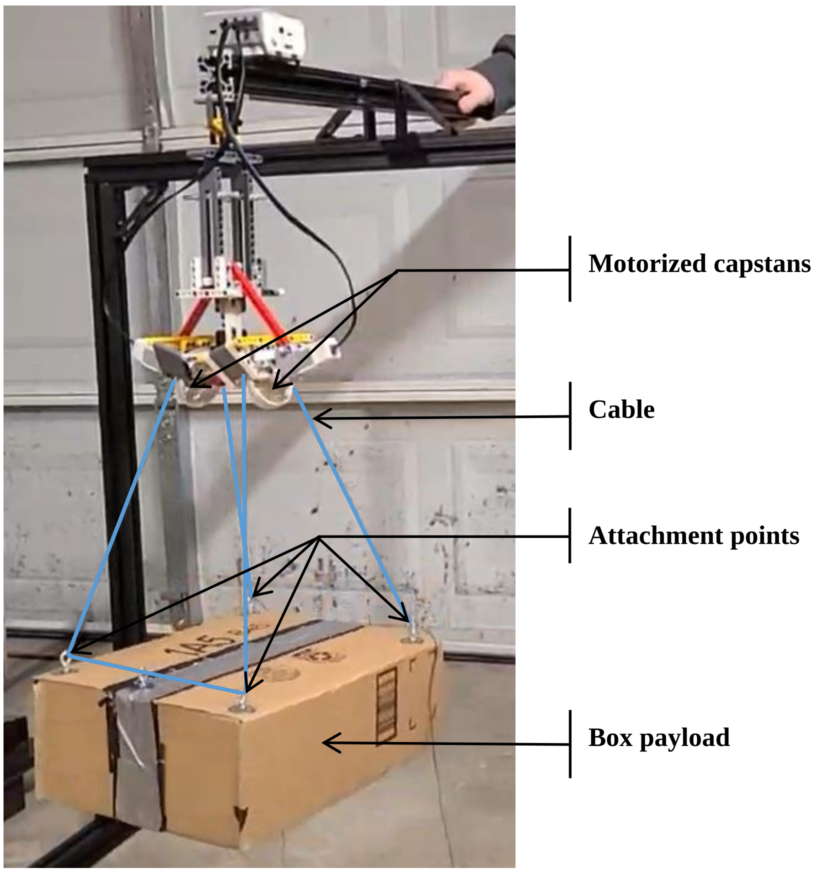

Figure 4. ARPHOLS LEGO prototype testing.

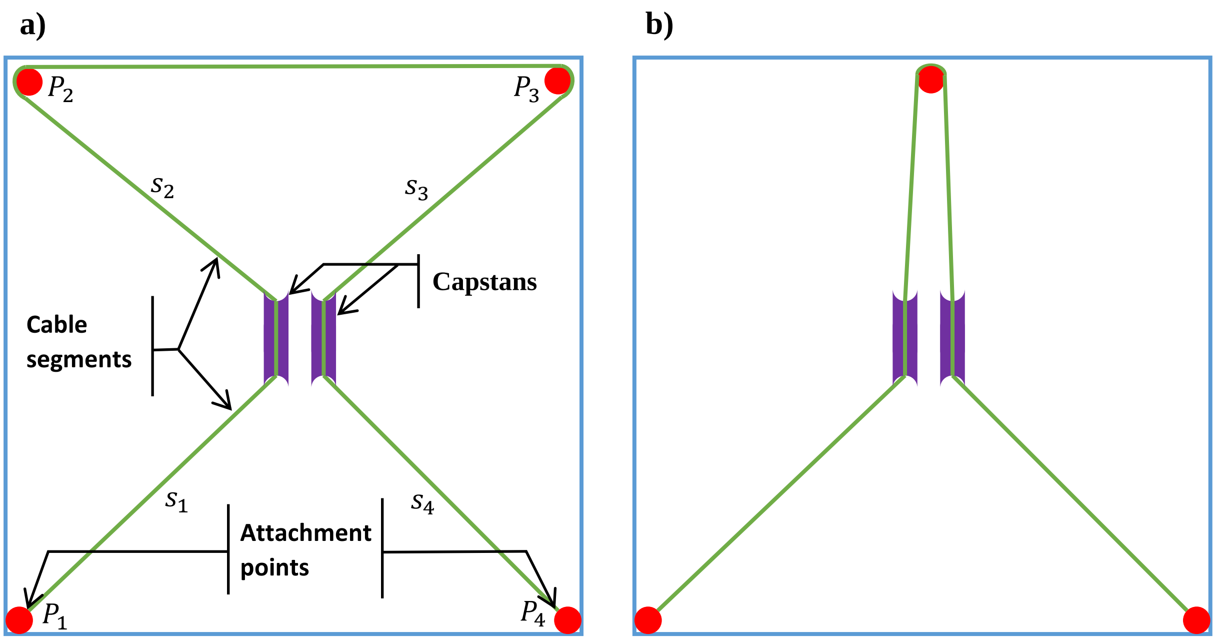

Figure 5. Payload top view for a) four attachment point configuration and b) three attachment point configuration.

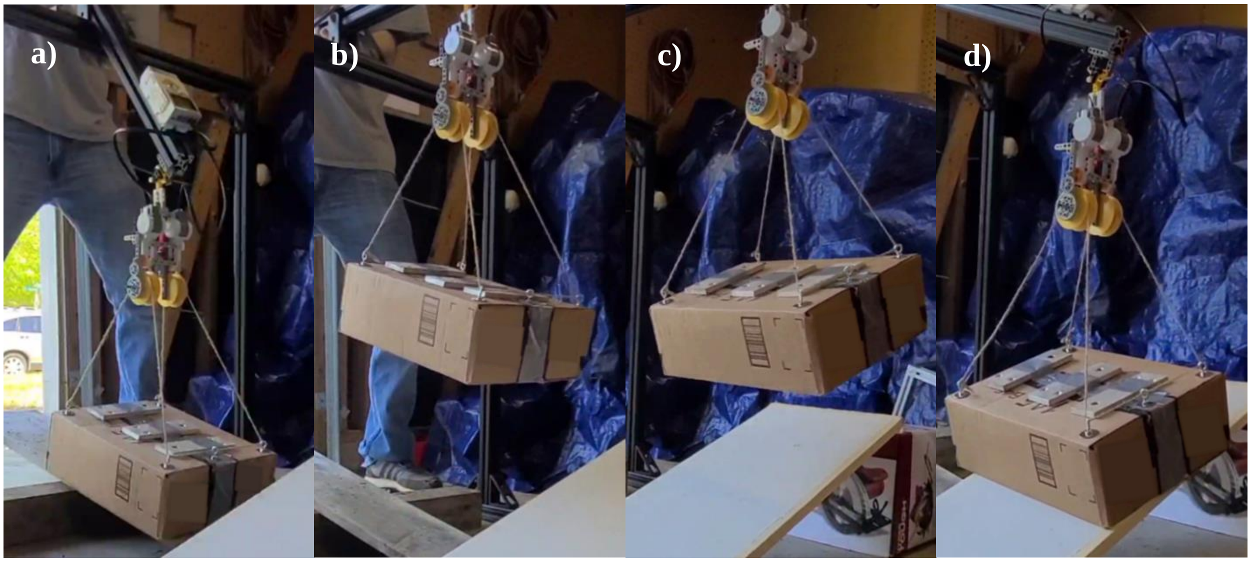

Figure 6. ARPHOLS prototype test sequence showing a) cable segments set to the required lengths for the payload to be in equilibrium prior to lifting, b) payload lifted in equilibrium, c) payload moved to the offloading site and the payload orientation adjusted to match the new incline, and d) payload offloaded.

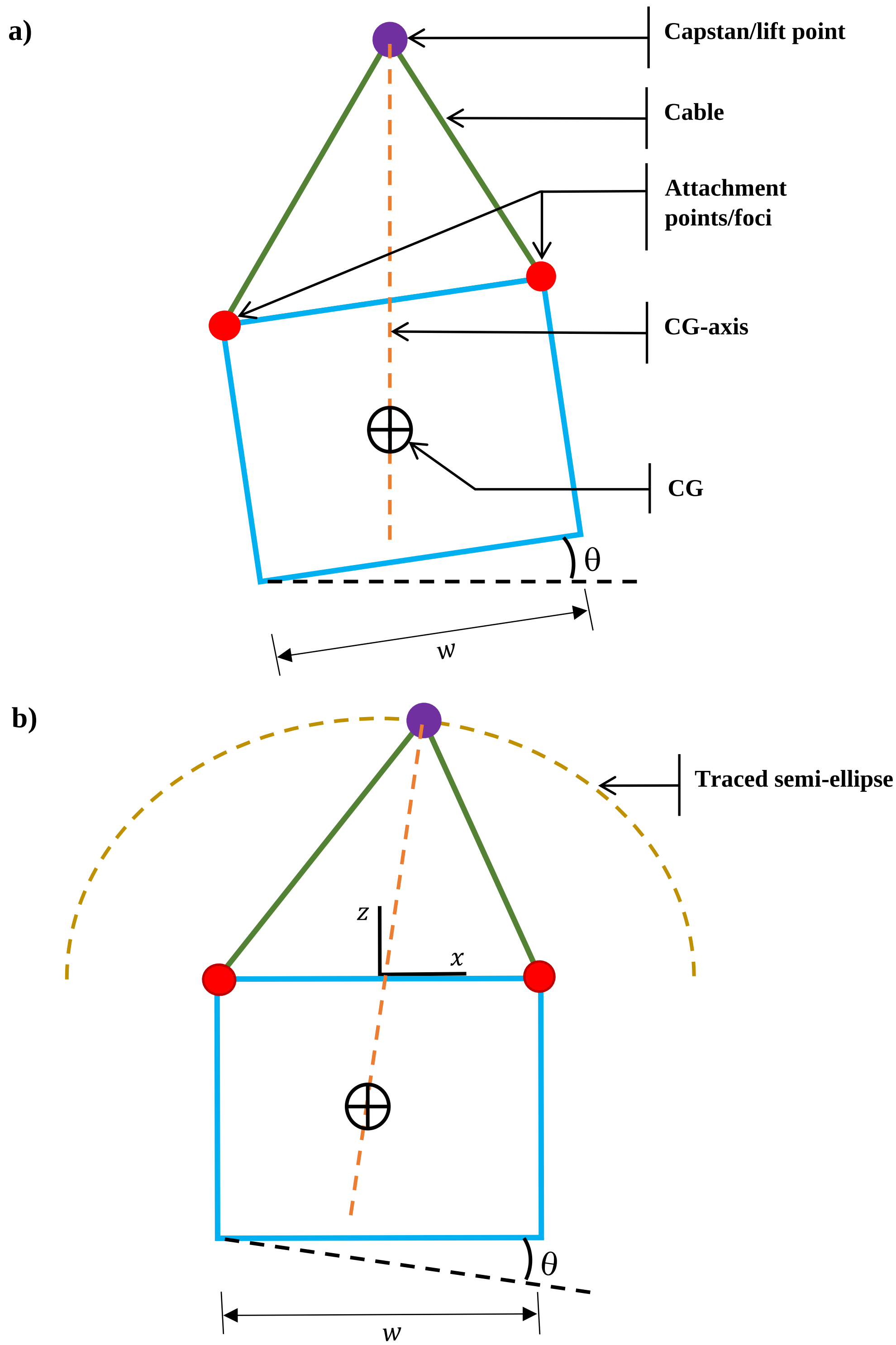

Figure 7. a) 2D model in the gravity reference frame with the origin fixed to the CG. b) 2D model in the payload reference frame with the origin fixed to the middle of the top of the payload. The capstan traces a semi-ellipse relative to the top of the payload as it rotates.

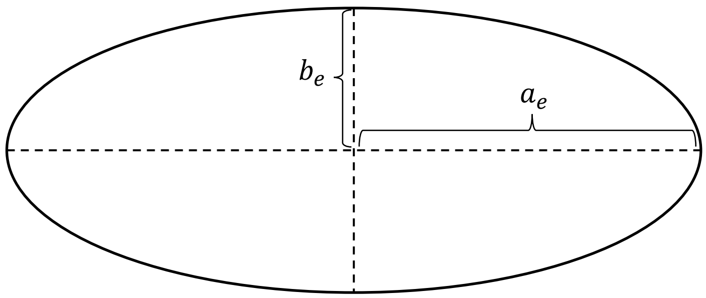

Figure 8. Ellipse with semiaxes labeled.

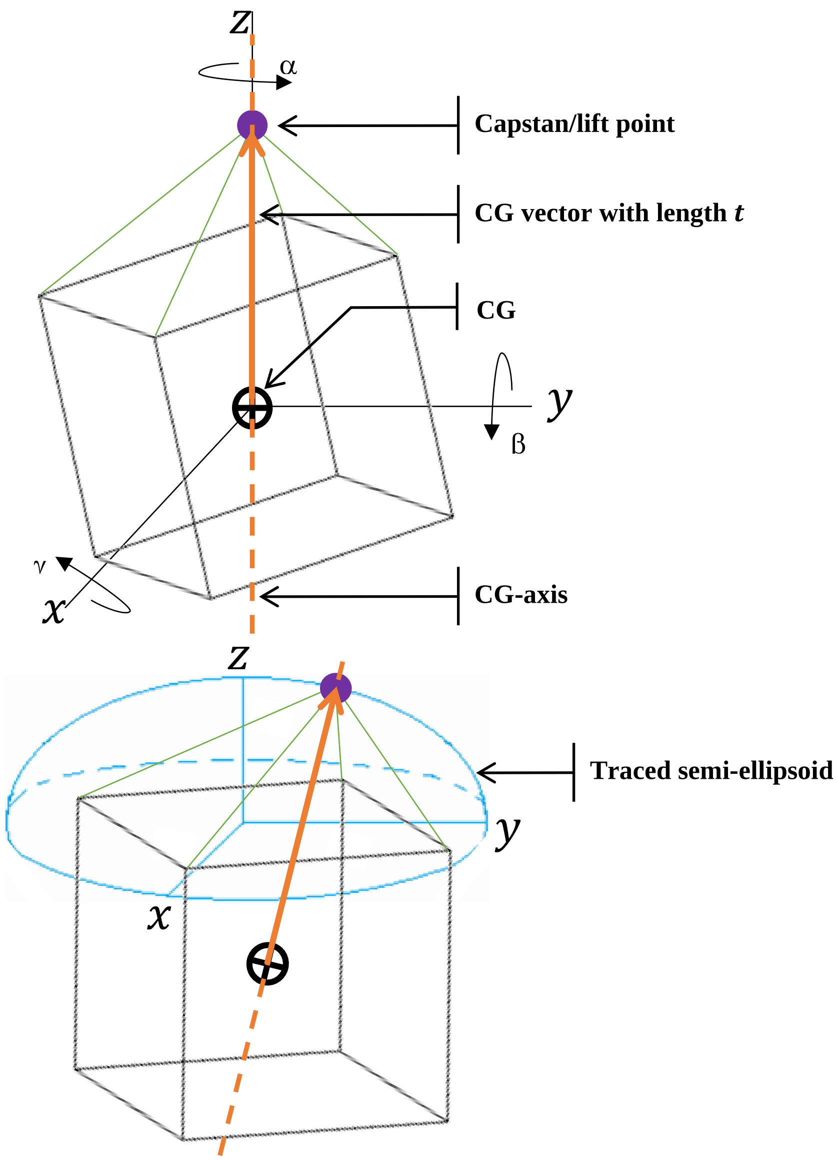

Figure 9. a) 3D model in the gravity reference frame with the origin fixed to the CG. Rotations are applied to the CG vector to transform it into the payload reference frame. b) 3D model in the payload reference frame with the origin fixed to the middle of the top surface of the payload. The capstan traces a semi-ellipsoid relative to the top of the payload as it rotates.

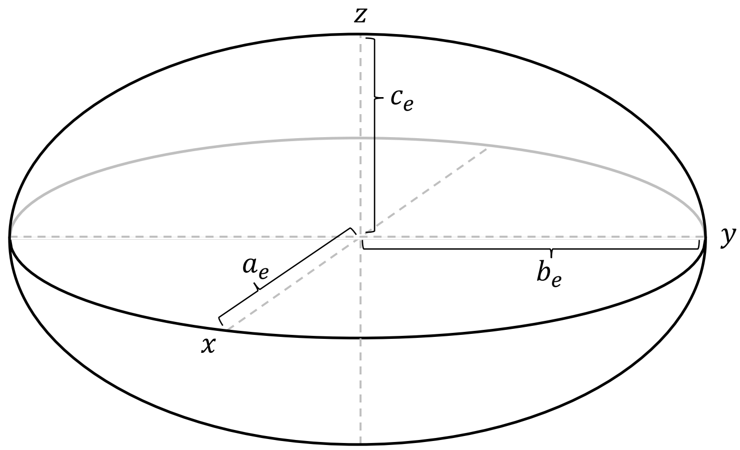

Figure 10. Ellipsoid with semiaxes labeled.

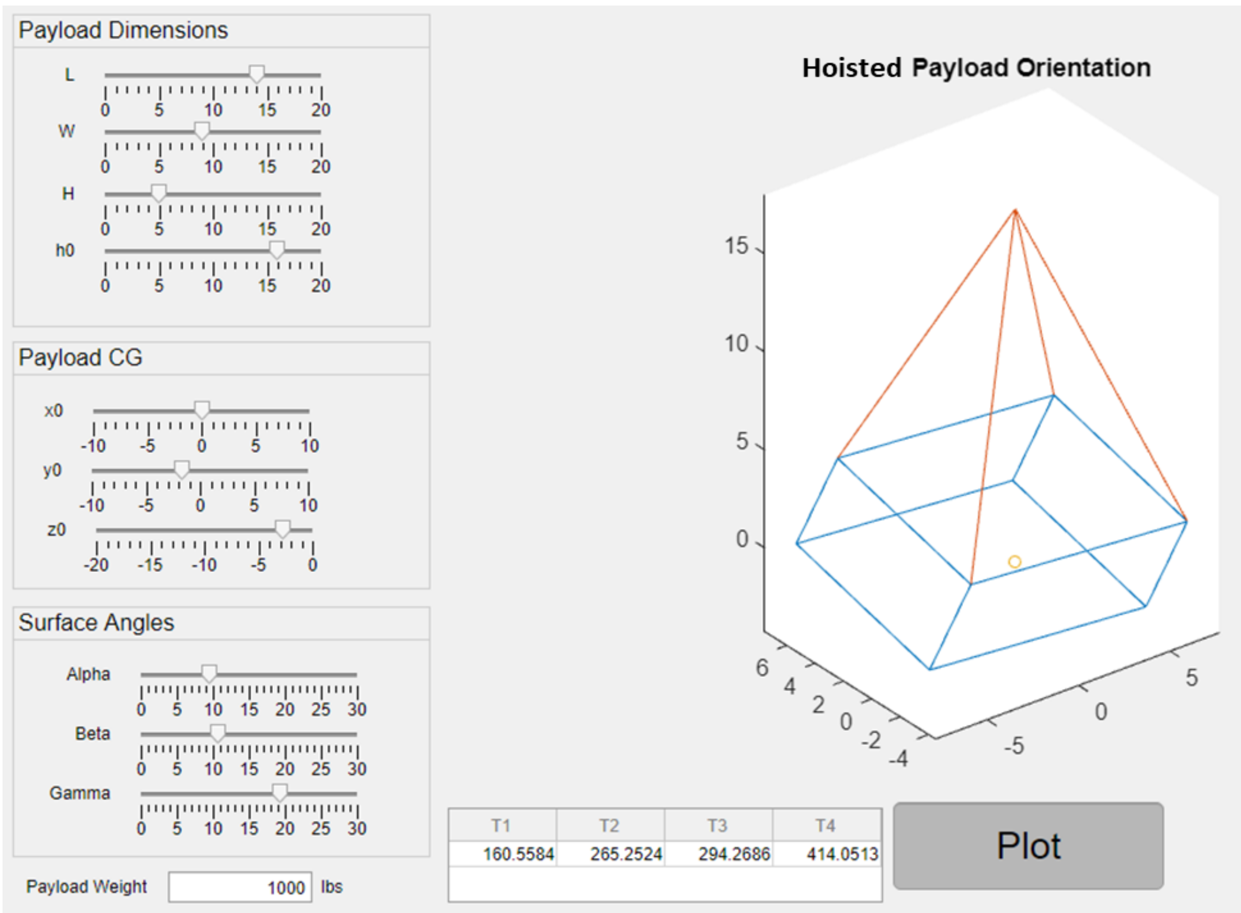

Figure 11. MATLAB app GUI that allows the user to adjust different payload parameters and incline angles. The resulting payload orientation is plotted, and the tensions (T1, T2, T3, and T4) in each cable segment are displayed.